Antigen Recognition Determinants of γδ T Cell Receptors

Sunny Shin,[1] Ramy El-Diwany,[1,2] Steven Schaffert,[1] Erin J. Adams,[1,2] K. Christopher Garcia,[1,2] Pablo Pereira,[3] Yueh-hsiu Chien[1,2]*

The molecular basis of γδ T cell receptor (TCR) recognition is poorly understood. Here, we analyze the TCR sequences of a natural γδ T cell population specific for the major histocompatibility complex class Ib molecule T22. We find that T22 recognition correlates strongly with a somatically recombined TCRδ complementarity-determining region 3 (CDR3) motif derived from germ line–encoded residues. Sequence diversity around these residues modulates TCR ligand-binding affinities, whereas V gene usage correlates mainly with tissue origin. These results show how an antigen-specific γδ TCR repertoire can be generated at a high frequency and suggest that γδ T cells recognize a limited number of antigens.

The γδ and αβ T cells contribute to host immune defense in distinct ways. Whereas αβ T cells are essential in pathogen clearance, γδ T cells have been implicated in the regulation of the immune response (*1*). Although it is clear that γδ T cells can recognize antigens directly without antigen processing and presentation requirements (*2*), it is unclear what the majority of γδ T cell ligands are and how they are recognized. This has made it difficult to define the precise function of γδ T cells. Previously, we found that the closely related major histocompatibility complex (MHC) class Ib molecules T10 and T22 (94% amino acid identity) are induced on activated cells and are ligands for a sizable population (~0.1% to 2%) of γδ T cells in unimmunized mice (*3*). This is potentially an important γδ T cell-ligand pair that could help to regulate immune cells. To understand how this antigen-specific repertoire is generated, particularly the high initial frequency of these cells, we used a T22 tetrameric staining reagent to identify and isolate T22-specific γδ T cells and determined their TCR sequences.

Most splenic γδT cells express Vγ1 and Vγ4, whereas Vγ7-expressing γδ T cells are more prevalent in the intestinal intraepithelial lymphocyte (IEL) compartment (*4*–*6*). This bias in Vγ usage has led to the suggestion that Vγ-encoded residues enable these T cells to respond to antigens unique to their resident tissues (*1*, *7*). Because T22-specific γδ T cells are present in both the spleen and IEL compartments, we first tested whether T22 specificity correlates with V gene usage (*8*). We found that multiple Vγs and Vδs are associated with T22-specific γδ T cells from these two tissues; however, the majority of T22 tetramer-positive cells express Vγ1 and Vγ4 in the spleen, whereas a sizable population of these cells express Vγ7 in the IEL compartment (Fig. 1A and table S1 and S3). This result indicates that Vγ usage is more reflective of the tissue origin than of the antigen specificity for this ligand.

We then compared the TCR sequences of individual T22 tetramer-positive and -negative cells (*8*). Although no conserved sequences in T22-specific TCRγ chains can be identified (tables S1 to S4 and fig. S1), we found that ~90% of the tetramer-positive IELs and ~40% to 60% of the splenic tetramer-positive TCRs contained a prominent CDR3δ sequence motif (Fig. 2A). This motif is also present in the T22-specific G8 and KN6 TCRs (*9*, *10*) but is absent from tetramer-negative splenic cells and more than 98% of the tetramer-negative IELs (tables S1 and S3). This motif consists of a tryptophan (W) encoded by the Vδ or Dδ1 gene segments and the sequence serine–glutamic acid–glycine–tyrosine–glutamic acid (SEGYE), followed by a P nucleotide–encoded leucine (L). Other than the motif, the CDR3δ sequences are diverse, encoded by various Vδs, N and P nucleotides, and Dδ1 in different lengths and reading frames. It is interesting that Vδ6A is the only Vδ to encode a tryptophan residue in the CDR3δ and is overrepresented in T22-specific γδ TCRs (Fig. 1B). Additionally, the CDR3δ length distribution is narrower and longer than that of γδ TCRs in general (Fig. 2, B and C).

To test whether TCRs derived from T22 tetramer-positive cells confer T22 binding specificity, we expressed several of these TCRs in the TCRβ-deficient Jurkat T cell line J.RT3-T3.5, which lacks endogenous surface TCR expression (*8*, *11*). We found that cells expressing TCRs that have the W-(S)EGYEL motif could bind T22 tetramer, whereas those that lack this motif could not (Fig. 3 and fig.

[1]Department of Microbiology and Immunology, [2]Program in Immunology, Stanford University School of Medicine, Stanford, CA 94305, USA. [3]Unité du Développement des Lymphocytes, Centre National de la Recherche Scientifique, Unité de Recherche Associée 1961, Institut Pasteur, 75724 Paris, France.

*To whom correspondence should be addressed. E-mail: chien@stanford.edu

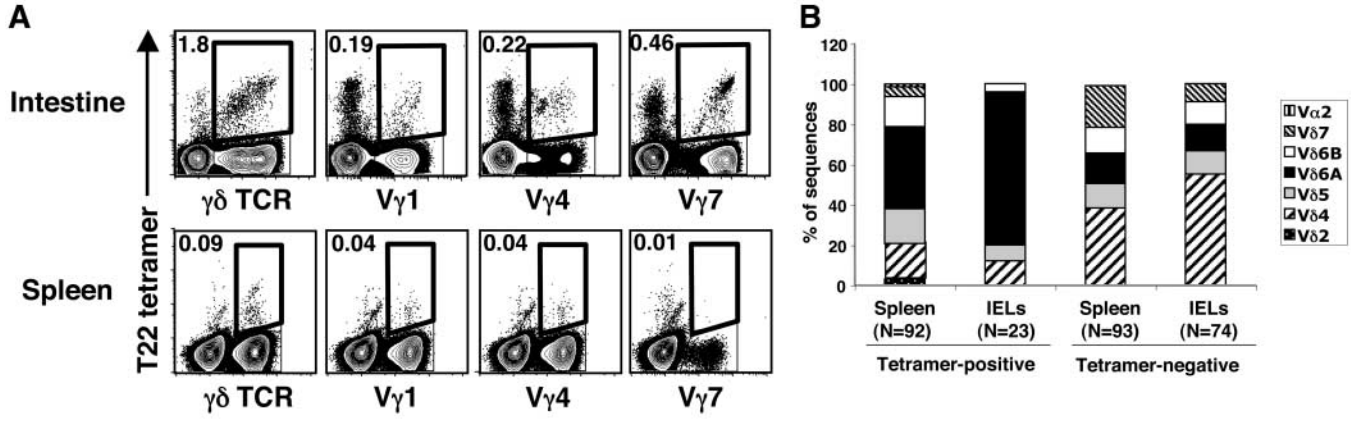

Fig. 1. (**A**) Staining of T22 tetramer with antibodies against Vγ1, Vγ4, and Vγ7 on splenic γδ T cells and IELs (antibodies to Vγ2, Vγ3, and Vγ6 are not available). Number within the plot indicates the percentage of total γδ T cells that are T22 tetramer-positive and Vγ-positive as shown in the box. (**B**) Relative frequency of Vδ usage of T22 tetramer-positive TCR sequences (tables S1 to S4) (*N* is total number of in-frame rearrangements analyzed).

S2). Thus, the higher rate of splenic tetramer-positive T cells without the TCRδ motif may be due to a higher false-positive rate in identifying these cells. This may be caused by the experimental limit associated with fluorescence-activated cell sorting (FACS), especially for low tetramer binders. (T22 tetramer stains IELs at a higher intensity than splenic cells.) Indeed, more recent experiments with a slightly more stringent FACS gating showed that ~70% of the splenic tetramer-positive cells have the TCRδ motif (*12*). Regardless, although both KN6 and 93A10 TCRs use a Vγ4-Vδ5 gene combination, only KN6 contains the W-(S)EGYEL CDR3δ motif and is T22-specific. G8 (Vγ4-Vα11.3), KN6 (Vγ4-Vδ5), as well as 93B7, 93D11, and 917B7 (Vγ1-Vδ6A), all bind T22 but use three different Vγ-Vδ pairs. This indicates that the W-(S)EGYEL CDR3δ motif correlates much better than V gene usage with antigen recognition. Consistent with this is the structural analysis of the G8-T22 complex showing that the residues W and GYEL in the G8 TCR CDR3δ are the principal T22 contact residues (*13*).

To test whether variability in the sequences surrounding the W-(S)EGYEL motif influences ligand binding, we compared the T22 binding characteristics of cells expressing similar levels of the 93B7, 93D11, and 917B7 TCRs, which differ only in those residues. As shown in Fig. 3, these TCRs exhibit significant differences in the half-life ($t_{1/2}$) and affinity (K_D) of T22 tetramer binding. Thus, sequence variations around this motif can modulate the affinity and the kinetics of ligand binding.

These results indicate that, for T22 specificity, a CDR3δ sequence generated by somatic rearrangement is necessary. This is similar to antibody specificities, which reside predominantly in the CDR3 of the heavy chain (*14*, *15*). Also, in the case of αβ TCRs, peptide-MHC specificity is determined largely by CDR3α and CDR3β, but the nature of the antigen-recognition determinants of T22-specific γδ TCRs and αβ TCRs are quite different. The T22-specific CDR3δ motif is encoded mainly by Dδ2 with contributions from Vδ, Dδ1, and P nucleotides, whereas in αβ TCRs the most critical residues for peptide-MHC recognition are encoded either completely or partially by N nucleotides in both CDR3α and CDR3β (*15*).

To determine whether a largely intact Dδ2 is a unique feature of T22-specific TCRs or of γδ TCRs in general, we analyzed the Dδ2 length distribution of in-frame thymocyte TCRδ sequences (N = 431). We found that ~23% of these sequences contain Dδ2 in its entirety, whereas an additional ~30% retain at least 13 out of 16 Dδ2 nucleotides (Table 1). A similar Dδ2 length distribution was also found in nonselected TCRs (N = 271) consisting of out-of-frame TCRδ chains and TCRδ rearrangements from CD3ε$^{-/-}$ thymocytes, which cannot express surface TCR (Table 1). This indicates that TCRδ rearrangements are strongly biased toward maintaining long Dδ2 regions. In the periphery, more than 50% of both the T22-specific and non–T22-specific splenic and IEL sequences contain Dδ2 in its entirety, and more than 70% of the sequences have less than three nucleotides deleted (Table 1), indicating that the resulting

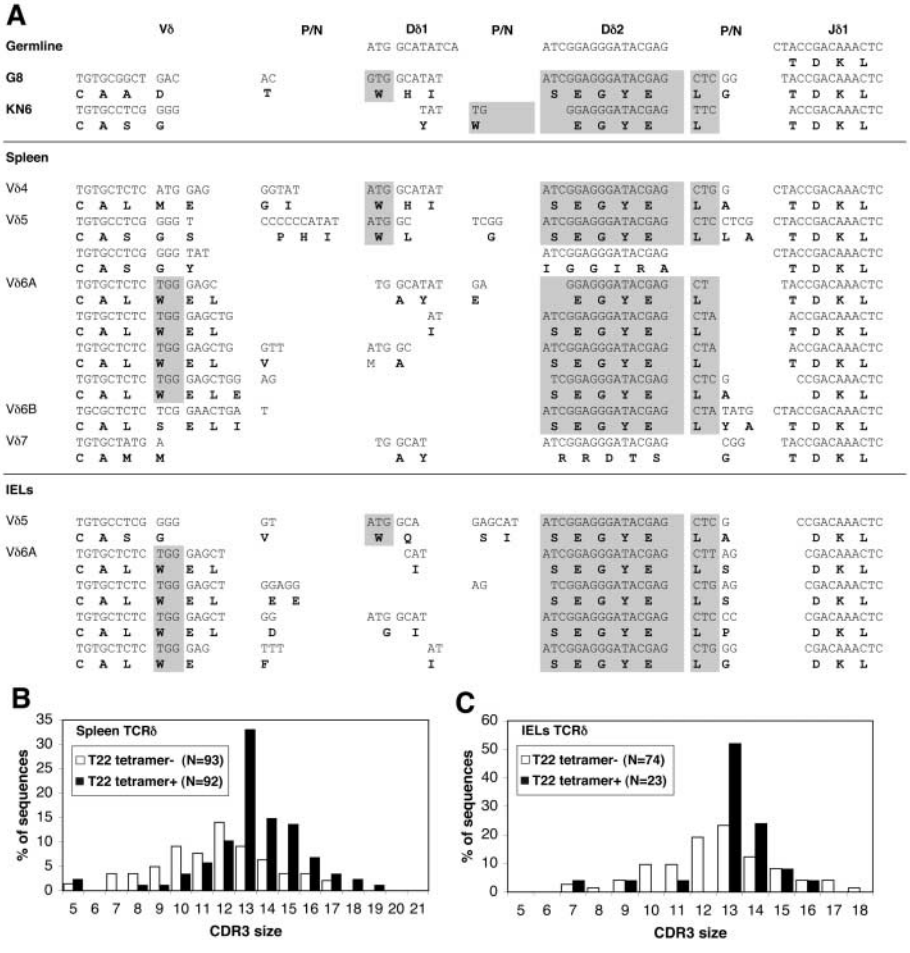

Fig. 2. (**A**) CDR3δ nucleotide and amino acid sequences from G8, KN6, and representative T22 tetramer-positive TCRs with the W-SEGYEL motif highlighted (*22*). CDR3δ size distributions for the (**B**) splenocyte and (**C**) IEL populations [calculated according to (*23*)] using productive rearrangements from the single cell sequence analyses (*N* is the total number of rearrangements analyzed).

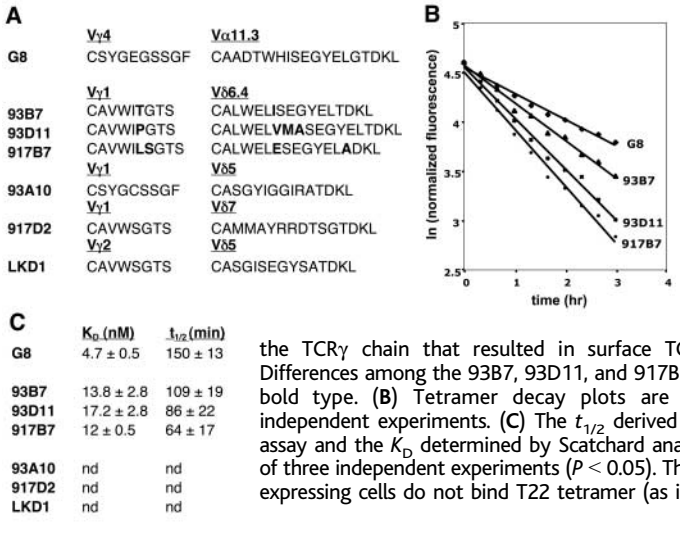

Fig. 3. (**A**) CDR3 sequences of G8, LKD1 (MHC class II I-A^d-specific), 93B7, 93D11, 917B7 (containing the W-SEGYEL motif), and 93A10 and 917D2 (not containing the motif) TCRs (*22*). The 93B7, 93D11, and 917B7 TCRs had two in-frame γ chain rearrangements (table S1). Only the sequence of the TCRγ chain that resulted in surface TCR expression is shown. Differences among the 93B7, 93D11, and 917B7 CDR3δ sequences are in bold type. (**B**) Tetramer decay plots are representative of three independent experiments. (**C**) The $t_{1/2}$ derived from the tetramer decay assay and the K_D determined by Scatchard analysis (*24*) are the average of three independent experiments ($P < 0.05$). The 93A10 and 917D2 TCR-expressing cells do not bind T22 tetramer (as indicated by nd).

TCRs are further selected for full use of the Dδ2 segment. In contrast, Dβ sequences from lymph node CD4+, Vβ17+ αβ T cells (*16*) show that only 3 to 7% are intact and fewer than 15 to 30% have been truncated by three nucleotides or less (Table 1).

Another feature distinguishing TCRδ CDR3 sequences from those of TCRβ and IgH chains is the J region. In both the TCRβ and the IgH chains, multiple J regions (12 Jβs and 6 J_Hs in mice) provide important framework residues and also contribute to antigen binding via their N-terminal residues (*15*). Exonuclease digestion and the addition of N nucleotides to the J region contribute to variability and thus to antigen binding (*15*). In contrast, adult murine γδ TCRs use only one Jδ, and the degree of exonuclease digestion is quite limited compared with αβ TCRs in that more than 98% of the sequences (T22-specific as well as nonspecific) retain the first or second N-terminal amino acid residue encoded by Jδ1 (Table 2). This very limited J region diversity is also found among thymocytes and nonselected γδ TCRs (Table 2), revealing yet another unique feature of TCRδ gene rearrangement. This relative lack of variation suggests that, unlike J_H and Jβ, Jδ1 does not play a major role in antigen recognition.

Although most γδ T cell ligands have yet to be identified, our observations indicate that rearrangements at the TCRδ locus are largely biased toward full-length Dδ2 sequences rather than extensive D-region nucleotide deletion, as is the case for the TCRβ locus. Thus, different reading frames of Dδ2 may contribute to the recognition of other ligands by γδ TCRs in a manner similar to that of T22-specific γδ TCRs. This would allow these germ line–encoded CDR3 sequences to coevolve with their ligands. In fact, most well-defined γδ T cells' ligands are self-molecules that could act as indicators of physiological disturbances, such as T10 and T22 in the mouse and MICA and B, CD1, and F1–adenosine triphosphate synthase in humans (*3*, *17*–*19*).

One would expect that a T cell repertoire generated from somatic recombination but whose specificity is conferred by germ line–encoded amino acids (such as for T22-specific γδ TCRs) would be created much more frequently than αβ T cells whose specificity is conferred primarily by N-nucleotide additions. In fact, we find that 0.85% of nonselected TCRδ sequences (N = 353) contain this CDR3δ motif (table S5) compared to one in 10^5 to 10^6 αβ T cells specific for a given peptide-MHC before clonal expansion (*20*, *21*). Thus, rearrangement alone could in part account for the high frequency (0.1 to 2%) of T22-specific γδ T cells in normal mice (Fig. 1A) (*3*, *12*). If γδ TCR specificity for other ligands is determined in a similar manner, then the γδ T cell repertoire must be directed against a relatively small number of ligands but with high frequency. This could allow for a rapid and significant response without an initial need for clonal expansion.

The CDR3δ provides the TCRδ with the highest potential diversity of all antigen receptor polypeptides. The results described here show that this diversity endows T22-specific γδ TCRs with different ligand-binding affinities. Indeed, the T22-specific TCR repertoire in normal mice covers a range of affinities, as evidenced by the large range of T22 tetramer-staining intensities (Fig. 1) (*3*, *12*). A self-reactive TCR repertoire with such diverse ligand-binding properties would enable more flexible and efficient responses to changes in self-ligand expression and at the same time allow for selection against high-affinity T cells that might respond inappropriately to basal ligand expression amounts.

Table 1. Dδ2 length distribution in TCRδ rearrangements. Numbers represent the percentage of rearrangements with the indicated number of nucleotides removed. The lengths of D regions were analyzed in nucleotides because they can be read in all three reading frames. Sequences analyzed are functional T22 tetramer-positive and -negative TCRδ chains (tables S1 to 4); functional TCRδ chains from γδ T cell hybridomas (*25*) and thymocytes (*26*) nonselected TCRδ chains from CD3$\varepsilon^{-/-}$ thymocytes (*25*), out-of-frame rearrangements from γδ T cell hybridomas, and single-cell analyses from thymocytes (*27*); and CD4+, Vβ17+ TCRβ chains from the lymph nodes of SJL mice (*15*) (*n* indicates the number of sequences analyzed).

Dδ/Dβ nucleotides deleted	Spleen		IEL		Functional TCRδ chains (n = 431) (%)	Nonselected TCRδ chains (n = 271) (%)	Vβ17+ CD4+ αβTCR Dβ1 (n = 37) (%)	Vβ17+ CD4+ αβTCR Dβ2 (n = 57) (%)
	Tetramer+ (n = 92) (%)	Tetramer– (n = 93) (%)	Tetramer+ (n = 23) (%)	Tetramer– (n = 77) (%)				
0	55.4	36.5	52.2	44.6	23	21.4	2.7	7
1−3	29.3	30.1	30.4	25.7	30.2	28	10.8	21.1
4−6	8.7	19.4	8.7	20.3	22.5	22.5	51.3	28.1
7−10	6.5	12.9	4.3	9.4	23	22.5	0	21
undetermined	0	1.1	4.3	0	1.4	5.5	35	22.8

Table 2. Jδ1 length distribution in TCRδ rearrangements. Numbers represent the percentage of rearrangements with the indicated number of amino acids (J region) removed. Sequences analyzed are functional T22 tetramer-positive and -negative TCRδ chains (tables S1 to 4); functional TCRδ chains from γδ T cell hybridomas (*25*) and thymocytes (*26*) nonselected TCRδ chains from CD3$\varepsilon^{-/-}$ thymocytes (*25*), out-of-frame rearrangements from γδ T cell hybridomas, and single-cell analyses from thymocytes (*27*); and CD4+, Vβ17+ TCRβ chains from the lymph nodes of SJL mice (*15*) (*n* indicates the number of sequences analyzed).

Jδ/Jβ amino acids deleted	Spleen		IEL		Functional TCRδ chains (n = 431) (%)	Nonselected TCRδ chains (n = 271) (%)	Vβ17+ CD4+ αβTCR Jβ (n = 75) (%)
	Tetramer+ (n = 92) (%)	Tetramer– (n = 93) (%)	Tetramer+ (n = 23) (%)	Tetramer– (n = 77) (%)			
0	69.1	79.4	23.1	80.5	68.4	71.3	34.7
1	30.9	19.6	76.9	18.2	26	22.8	44
2	0	1	0	1.3	5.6	5.9	16
3 or more	0	0	0	0	0	0	7

References and Notes

1. A. C. Hayday, *Annu. Rev. Immunol.* **18**, 975 (2000).
2. Y-h. Chien, R. Jores, M. P. Crowley, *Annu. Rev. Immunol.* **14**, 511 (1996).
3. M. P. Crowley *et al.*, *Science* **287**, 314 (2000).
4. P. Pereira, D. Gerber, S. Y. Huang, S. Tonegawa, *J. Exp. Med.* **182**, 1921 (1995).
5. A. I. Sperling, R. Q. Cron, D. C. Decker, D. A. Stern, J. A. Bluestone, *J. Immunol.* **149**, 3200 (1992).
6. D. M. Asarnow, T. Goodman, L. LeFrancois, J. P. Allison, *Nature* **341**, 60 (1989).
7. C. A. Janeway Jr., B. Jones, A. Hayday, *Immunol. Today* **9**, 73 (1988).
8. Materials and methods are available on *Science* Online.
9. M. Bonneville *et al.*, *Proc. Natl. Acad. Sci. U.S.A.* **86**, 5928 (1989).
10. J. A. Bluestone, R. Q. Cron, M. Cotterman, B. A. Houlden, L. A. Matis, *J. Exp. Med.* **168**, 1899 (1988).
11. P. S. Ohashi *et al.*, *Nature* **316**, 606 (1985).
12. S. Shin *et al.*, unpublished data.
13. E. A. Adams, Y. Chien, K. C. Garcia, *Science* **308**, 227 (2005).
14. J. L. Xu, M. M. Davis, *Immunity* **13**, 37 (2000).
15. M. M. Davis, Y. Chien, in *Fundamental Immunology*, W. E. Paul, Ed. (Lippincott, Philadelphia, 2003).
16. S. Candeias, C. Waltzinger, C. Benoist, D. Mathis, *J. Exp. Med.* **174**, 989 (1991).
17. J. Wu, V. Groh, T. Spies, *J. Immunol.* **169**, 1236 (2002).
18. F. M. Spada *et al.*, *J. Exp. Med.* **191**, 937 (2000).
19. E. Scotet *et al.*, *Immunity* **22**, 71 (2005).
20. M. G. McHeyzer-Williams, M. M. Davis, *Science* **268**, 106 (1995).
21. P. Bousso *et al.*, *Immunity* **9**, 169 (1998).

22. Single-letter abbreviations for the amino acid residues are as follows: A, Ala; C, Cys; D, Asp; E, Glu; F, Phe; G, Gly; H, His; I, Ile; K, Lys; L, Leu; M, Met; N, Asn; P, Pro; Q, Gln; R, Arg; S, Ser; T, Thr; V, Val; W, Trp; and Y, Tyr.

23. E. P. Rock, P. R. Sibbald, M. M. Davis, Y. H. Chien, *J. Exp. Med.* **179**, 323 (1994).
24. P. A. Savage, J. J. Boniface, M. M. Davis, *Immunity* **10**, 485 (1999).
25. P. Pereira *et al.*, *Eur. J. Immunol.* **30**, 1988 (2000).
26. V. Azuara, M. P. Lembezat, P. Pereira, *Eur. J. Immunol.* **28**, 3456 (1998).
27. P. Pereira, L. Boucontet, *J. Immunol.* **173**, 3261 (2004).
28. We thank M. Davis for critical review of the manuscript; Y. Konigshofer, K. Jensen, M. Krogsgaard, M. Kuhns, J. Huppa, R. Sciammas, and I. Brodsky for advice and reagents; L. Boucontet for technical assistance; and L. Lefrancois and L. Puddington for the antibody against Vγ5. Supported by NIH grant AI33431 (Y.-h.C.), the Association pour la Recherche sur le Cancer (P.P.), a Stanford Immunology training grant fellowship (E.J.A.), a National Institute of Allergy and Infectious Diseases Richard A. Asofsky Research Award (R.E.-D.), and an NSF predoctoral fellowship (S.S.).

Supporting Online Material
www.sciencemag.org/cgi/content/full/308/5719/252/DC1
Materials and Methods
Figs. S1 to S3
Tables S1 to S5
References

18 October 2004; accepted 15 February 2005
10.1126/science.1106480

Do 15-Month-Old Infants Understand False Beliefs?

Kristine H. Onishi[1]* and Renée Baillargeon[2]

For more than two decades, researchers have argued that young children do not understand mental states such as beliefs. Part of the evidence for this claim comes from preschoolers' failure at verbal tasks that require the understanding that others may hold false beliefs. Here, we used a novel nonverbal task to examine 15-month-old infants' ability to predict an actor's behavior on the basis of her true or false belief about a toy's hiding place. Results were positive, supporting the view that, from a young age, children appeal to mental states—goals, perceptions, and beliefs—to explain the behavior of others.

Consider the following situation: A child who has surreptitiously eaten the last cookies in a box sees her brother reach into the box. To make sense of his behavior, she must understand that he falsely believes the box still contains cookies. As adults, we readily understand that others may hold and act on false beliefs; this ability is widely held to be a cornerstone of social competence, and its neuronal correlates have recently begun to be examined (*1*). What are the origins of this ability? Within the field of psychology, there has been a longstanding controversy regarding this issue (*2–4*).

Some researchers have suggested that at about 4 years of age a fundamental change occurs in children's understanding of others' behavior, or "theory of mind": They begin to realize that mental states such as beliefs are not direct reflections of reality, which must always be accurate, but representations, which may or may not be accurate (*5–8*). Part of the evidence for this change from a nonrepresentational to a representational theory of mind has come from young children's well-documented failure at false-belief tasks (i.e., tasks that require the understanding that others may hold and act on false beliefs) (*9–13*). In a standard task (*10*), children listen to a story as it is enacted with dolls and toys: The first character hides a toy in one location and leaves the room; while she is gone, a second character hides the toy in a different location. When asked where the first character will look for her toy, 4 year olds typically say she will look in the first location and provide appropriate justifications for their answers. In contrast, most 3 year olds say she will look in the second (actual) location, thus failing to demonstrate an understanding that the first character will hold a false belief about the toy's location.

Other researchers have suggested that a representational theory of mind is present much earlier and that young children's difficulties with the standard false-belief task stem primarily from excessive linguistic, computational, and other task demands (*14–18*). Support for these claims comes in part from evidence that 3 year olds and even some 2 year olds succeed at a modified false-belief task (*19*, *20*). In this version of the task, after listening to the story and watching it enacted, children are simply probed by the experimenter to look where the first character will search for her toy upon her return ("I wonder where she will look"). Most children look to the correct location, suggesting that they possess some implicit understanding that others may hold and act on false beliefs. We examined whether 15-month-old infants tested with a simpler, entirely nonverbal task would also show some implicit understanding of false belief.

We used the violation-of-expectation method, which has been used extensively to investigate infants' understanding of others' goals (*21–23*). For example, in one experiment (*22*), infants were familiarized with an actor reaching for and grasping one of two toys (defined as the target toy). Next, the locations of the two toys were reversed, and the actor reached for the target or the nontarget toy. The infants looked reliably longer at nontarget reaches. This and control results suggested that the infants encoded the target toy as the actor's goal object, expected her to reach for it in its new location, and responded with increased attention when she did not. Similar results were found when the target toy was hidden rather than visible and was retrieved by means-end action sequences rather than by a simple reach (*23*). Our research built on these results. In our experiment, 15-month-old infants first watched an actor hide a toy in one of two locations. Next, a change occurred that resulted in the actor holding either a true or a false belief about the toy's location. The experiment asked whether the infants would expect the actor to search for her toy based on her belief about its location, whether that belief was true or false.

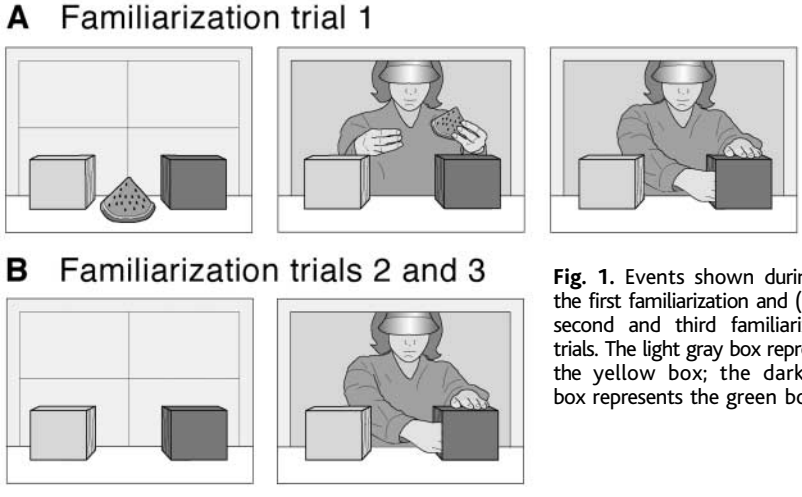

Fig. 1. Events shown during (**A**) the first familiarization and (**B**) the second and third familiarization trials. The light gray box represents the yellow box; the dark gray box represents the green box.

[1]Department of Psychology, McGill University, Montreal, Quebec H3A 1B1, Canada. [2]Department of Psychology, University of Illinois, Champaign, IL 61820, USA.

*To whom correspondence should be addressed. E-mail: kris.onishi@mcgill.ca